STEM CELLS TRANSLATIONAL MEDICINE®

TISSUE-SPECIFIC PROGENITOR AND STEM CELLS

Topical Application of Culture-Expanded CD34+ Umbilical Cord Blood Cells from Frozen Units Accelerates Healing of Diabetic Skin Wounds in Mice

JENNIFER WHITELEY,[a] THERESA CHOW,[a,b] HIBRET ADISSU,[a] ARMAND KEATING,[c] IAN M. ROGERS [a,b,d]

Key Words. Umbilical cord blood • Diabetes • Skin ulcer • Stem cells

[a]Lunenfeld Tanenbaum Research Institute, Sinai Health System, Toronto, Ontario, Canada; [b]Department of Physiology, University of Toronto and [c]Krembil Research Institute, Cancer Clinical Research Unit (CCRU), Princess Margaret Cancer Centre, Cell Therapy Program, Princess Margaret Hospital, Toronto, Ontario, Canada; [d]Division of Reproductive Sciences, Department of Obstetrics and Gynecology, Toronto, Ontario, Canada

Correspondence: Ian M. Rogers, Ph.D., Rm. 5-1015A Lunenfeld-Tanenbaum Research Institute, Sinai Health System, 25 Orde Street, Toronto, M5G 1X5, Ontario, Canada. Telephone: 416-586-4800 x 4122; e-mail: rogers@lunenfeld.ca

Received December 21, 2017; accepted for publication March 29, 2018; first published May 12, 2018.

http://dx.doi.org/10.1002/sctm.17-0302

ABSTRACT

Chronic and nonhealing wounds are constant health issues facing patients with type 2 diabetes. As the incidence of type 2 diabetes mellitus (T2DM) increases, the incidence of chronic wounds and amputations will rise. T2DM is associated with peripheral arterial occlusive disease, which leads to the development of nonhealing skin ulcers after minor trauma. Patients develop severe pain limiting their mobility and ability to work and take care of themselves, thus putting a significant burden on the family and society. CD34+ cells from umbilical cord blood (UCB) grown in fibroblast growth factor-4 (FGF-4), stem cell factor, and Flt3-ligand produced a population of cells that have the ability to proliferate and develop properties enabling them to enhance tissue regeneration. The goal of this study was to assess in vitro cultured CD34+ cells in a setting where they would eventually be rejected so we could isolate paracrine signaling mediated therapeutic effect from the therapeutic effect due to engraftment and differentiation. To achieve this, we used db/db mice as a model for diabetic skin ulcers. Here, we report that in vitro cultured UCB CD34+ cells from frozen units can accelerate wound healing and resulted in the regeneration of full thickness skin. This study demonstrates a new indication for banked UCB units in the area of tissue regeneration. STEM CELLS TRANSLATIONAL MEDICINE *2018;7:591–601*

SIGNIFICANCE STATEMENT

This study demonstrates that therapeutic cells from frozen umbilical cord units can be expanded ex vivo and retain their therapeutic properties. The cells were used to treat diabetic skin ulcers and demonstrated faster wound closure and improved skin regeneration compared to controls.

INTRODUCTION

Patients with type 2 diabetes mellitus (T2DM) are susceptible to nonhealing wounds due to a reduced number of keratinocytes and fibroblasts, including a reduction in their migration capabilities resulting in a prolonged inflammatory phase, increased apoptosis, and decreased vascularization. Normal wound healing is initiated by neutrophil migration and platelet activation after exposure to the wound during bleeding resulting in a fibrin clot being formed. The subsequent release of cytokines that promote inflammation and leukocyte migration to the injury site is important for recruiting macrophages to clean up debris, keratinocytes to initiate wound closure and fibroblasts to repair the underlying dermis and promote angiogenesis [1]. Diabetes alters the timing and duration of these events resulting in delayed early inflammation followed by increased macrophage and neutrophil infiltration at later stages. This results in the increased secretion of pro-inflammatory cytokines. Furthermore, during T2DM, there is evidence that diabetes maintains M1 macrophages, responsible for inflammation at the expense of supporting the recruitment of M2 macrophages, which secrete factors important for wound closure and angiogenesis [2, 3].

Keratinocytes that are normally activated to proliferate and migrate during wound healing are negatively affected by diabetes as migration associated proteins are downregulated. Endothelial cells and angioblast proliferation and migration are also negatively affected [4, 5]. Along with myofibroblasts, these cells are a major source of new extracellular matrix (ECM) that in turn provide the structure for new dermal tissue and contractile tissue required to stabilize and close the wound. The new ECM is modeled by matrix metalloproteinases (MMPs) and tissue inhibiting

metaloproteinases (TIMPs). Similar amounts of MMPs and TIMPs are optimal for tissue regeneration, but diabetes increases the expression of MMPs and decreases TIMPs resulting in reduce amounts and quality of ECM [6].

Studies using a variety of different cells have demonstrated that the addition of exogenous healthy cells can override the diabetes phenotype and enhance the regeneration of skin wounds [7, 8]. For example, using rodent models of diabetic skin ulcers, it has been demonstrated that the therapeutic ability of blood cells, in part, is due to the CD34+ cell population [5, 9]. CD34+ cells comprise hematopoietic stem cells, endothelial precursor cells (EPC), and circulating angiogenic cells (CAC) [10]. The latter two demonstrated strong paracrine signaling that promoted tissue regeneration. The main hurdle to using CD34+ blood cells is their low number. Umbilical cord blood (UCB) CD34+ cells make up less than 0.5% of all mononucleated cells and even less in peripheral blood and bone marrow [11]. To circumvent the problem of low CD34+ cell numbers in a UCB unit, we developed a method to proliferate these cells from frozen units [12, 13]. It was important to demonstrate the efficacy of frozen units since available UCB units are stored frozen in public and private banks.

UCB is an ideal source of therapeutic cells as UCB units are easily obtained, easily stored, and are a source of very young cells. It has been previously reported that mesenchymal stromal cells from bone marrow (BM-MSC) can enhance skin wound regeneration [14]. Although MSC-like cells can be obtained from UCB, the yield of these cells was low with only 50% of the units yielding viable cells if they were processed within 15 hours of collection. Furthermore, only 10% of frozen UCB resulted in viable MSC-like cells [15–18]. Similarly, the recovery of EPC was high from fresh UCB units (94%) but only 59% of frozen units [19, 20]. Thus, we sought out an alternative cell source from UCB that could be therapeutic [12, 13, 21]. We developed and described a methodology to isolate highly therapeutic cells that can be recovered from 100% of the frozen UCB units. These cells are described elsewhere but in summary they are not MSC but CD34+ blood cells that have the ability to enhance tissue regeneration mainly through paracrine signaling [21]. Being able to provide healthy donor cells from frozen, banked UCB units is important since studies have determined that age and disease state can adversely affect the ability of autologous cells to contribute to tissue repair [4, 22–24].

We focused on CD34+ cells due to their reported therapeutic ability. Our culture conditions resulted in an expansion of the total number of CD34+ cells. CD34+ cells were isolated from frozen banked units of UCB and grown in media supplemented with fibroblast growth factor-4 (FGF4), stem cell factor (SCF), and Flt3-ligand (FLT-3L). In previous studies, we have reported on the regenerative capacity of in vitro grown UCB-CD34+ cells. We refer to the cultured cells as multipotential stem cells (MPSC). In a peripheral vascular disease (PVD) model using NOD/SCID mice, we demonstrated the paracrine signaling of the MPSC had a major role in tissue repair, along with the ability of the cells to engraft and differentiate into endothelial cells and smooth muscle cells [21]. In a nonmatched model for spinal cord injury, where engraftment did not occur, we demonstrated that the paracrine signaling alone was capable of reducing secondary injury and improve the mobility of the injured mice [25]. MPSC also showed regenerative properties when used in a model of bone regeneration [26]. In the nonmatch setting, despite the fact the cells are short lived, a positive effect is observed beyond the life of the donor cells suggesting that the cells trigger a cascade of events that helps to restore normal wound healing.

Materials and Methods

UCB Cell Collection and Cell Preparation

Written consent for collecting and processing UCB was obtained at the time of registration for the study. Qualified hospital personnel, following protocols approved by the human ethics committee of the Mt. Sinai Hospital, collected UCB at the time of delivery. Pentastarch (Dupont, Wilmington, USA) was added (1:5) and the sample spun at 50*g* for 10 minutes at 10°C to sediment the red blood cells (RBC). The leukocyte rich plasma was centrifuged at 400*g* for 10 minutes at 10°C to pellet the cells. The cell pellet was resuspended in Iscoves Modified Dulbeccos Medium (IMDM) containing 10% serum and mixed with an equal volume of cryoprotectant (20% Dimethyl Sulfoxide/80% serum (heat inactivated/filtered), step frozen and stored in liquid nitrogen until required [12].

MPSC from UCB

Our method to produce MPSC from frozen samples of UCB is described in detail in other publications [12, 21, 25] and summarized here. We used either the Miltenyi-MACS CD34+ selection kit, Bergisch, Germany or the Stem Cell Technologies Stem-Sep kit, Vancouver, Canada to isolate CD34+ cells. CD34+ content was assessed using flow cytometry. The dead cell removal kit was used prior to CD34+ selection. Only frozen UCB units were used. Prior to the processing with the dead cell removal kit and selection, frozen units were filtered through a 70 micron mesh after thawing to remove clumps of dead cells that may have accumulated during the freeze/thaw process. Post column cells were seeded at 1×10^5 cells/ml in FSFl medium (StemSpan media [Stem Cell Technologies] containing IMDM, 1% bovine serum albumin (BSA), 10 mg/ml insulin, 200 mg/ml human transferrin, 10^{-4} M 2-mercaptoethanol, and 2 mM L-glutamine. The media was supplemented with 25 ng/ml SCF [R&D Systems, Minneapolis, MN], 25 ng/ml Flt-3 ligand [FL; R&D Systems, Minneapolis, MN] and 50 ng/ml Fibroblast Growth Factor-4 [FGF-4; R&D Systems, Minneapolis, MN], 50 ng/ml heparin and 10mg/ml low density lipoprotein [Sigma, Markham, Canada]). Fifty percent medium replacement occurred every 48 hours. For all animal experiments described here, the cells were used directly after 7–8 day culture in FSFl medium.

Flow Cytometry Analysis

Samples were stained with antibodies to CD34, CD38, and CD45 (Beckman-Coulter, Burlington, Canada) and subjected to flow cytometer analysis; Coulter-Epics (Coulter. Burlington, Canada). Isotype controls were used in all cases. All samples were labeled for 10–20 minutes at 4°C, washed, and fixed in 10% formalin, as per manufacturer's instructions.

BM-MSC Isolation

Written consent for collecting BM cells was obtained at the time of registration for the study. Qualified hospital personnel, following protocols approved by the human ethics committee of the Princess Margaret Hospital, Toronto, collected bone marrow aspirate from consented patients. Heparinized bone

marrow was mixed with a double volume of phosphate-buffered saline (PBS) and centrifuged at 900*g* for 10 minutes at room temperature. Washed cells were resuspended in PBS at 1×10^8 cells/ml and layered over a 1.073 g/ml on Ficoll solution and centrifuged at 900*g* for 30 minutes. Mononuclear cells were collected, washed, and resuspended in PBS and centrifuged at 900*g* for 10 minutes at 20°C. Cells were suspended in alpha Modified Eagles Medium (αMEM) (Life technologies, Gaithersburg, MD, USA), supplemented with 5% fetal bovine serum (FBS) and 1% antibiotic-antimycotic solution (Life technologies) and plated at 3×10^7 cells/175 cm^2. Cultures were maintained at 37°C in a humidified atmosphere containing 5% CO_2. When cultures reached 80% confluence, cells were detached with 0.25% trypsin (GibcoBRL, Grand Island, NY, USA) and replated (passaged) at 1×10^6 cells/175 cm^2. Medium was changed twice weekly.

In Vivo Studies

Wound Healing Model for Transplantation. Animals were cared for and handled in accordance with the Canadian Council on Animal Care and institutional guidelines (Toronto Centre for Phenogenomics). db/db male mice (BKS.Cg-*Dock7*^{m} +/+ *Lepr*^{db}/J Stock No: 000642, Jackson Labs, Bar Harbor, USA) were ordered in at 10 weeks of age and left for 2 weeks to acclimatize. Cages were changed daily due to excessive urination caused by diabetes symptoms. A splinted excisional wound model was used. Mice were induced and maintained on Isoflurane anesthesia. An injection of buprenorphine was administered subcutaneously before the procedure at a dose of 0.1 mg/kg. We choose to use buprenorphine because it lacks anti-inflammatory properties. The dorsal surface of the mouse was shaved and a depilatory cream was applied to completely remove the fur for better adherence of the splint and Tegaderm. A donut shaped splint with an inner diameter of 12 mm (0.5 mm silicone sheeting Grace Biolabs, Bent, USA) was placed. A bonding adhesive (Vetbond, Maplewood, USA) was used to fix the splint to the surrounding skin and 4 6-0 silk sutures was placed around the silicon splint to help hold the splint in place. A single full thickness wound (including the panniculosus carnosus) was created within the positioned splint using a sterile disposable 6 mm biopsy punch. Cells were applied to the surface of the wound (overlay) or injected around the wound edge (1–3 million/20 µl) then covered with 20 µl of fibrin. The fibrin was made just before use by mixing equal amounts of fibrinogen and thrombin and transparent Tegaderm was placed over the splint. Control animals received the vehicle of IMDM with 10% FBS followed by fibrin and a tegaderm covering.

Monitoring of the Wound. Wounds were monitored by taking digital photos at day 0, 3, 7, and 14 using the Canon Powershot SX150IS, Toronto, Canada. Photos were taken with the transparent Tegaderm dressing in place. Animals were restrained by placing them on the grid of the cage and held by the base of the tail. The silicon splints were used as a size reference when analyzing. Pictures were analyzed by drawing around the wound margins and measuring pixel area using Image J.

Tissue Collection and Processing

At day 7, 14, and 23, mice were euthanized by CO_2 and tissues were collected. The entire wound area and surrounding tissue (including muscle layer below the subcutaneous layer) was excised and placed in 10% neutral buffered formalin (NBF) for 16 hours, washed in PBS, and then stored in 70% EtOH. Tissues were routinely processed and embedded in paraffin. Tissues were sectioned through the center of the wound and 5 µm sections were prepared for routine H&E, Masson Trichrome, Sirius Red stains, and immunohistochemistry. Slides were visualized using a Hamamatsu Nanozoomer 2.0RS whole slide scanning system at ×20 (0.46 µm/pixel) with the Nanozoom Digital Pathology view (NDP.view2) software, Hamamatsu, Japan. Pictures are at magnification ×1.25 or ×14. Some tissue sections were photographed on a black background prior to fixing to illustrate the thickness of the closure.

Immunohistochemisty

Nonspecific binding was blocked with 10% serum in PBS containing 0.1% Triton X-100 (Sigma) for 240 minutes at room temperature. After a brief wash in PBS after the blocking, primary antibody was applied (solution 1:100) for overnight incubation at 4°C. Sections with omitted primary or secondary antibody were used as another type of negative control in each experiment. After five washes for 15 minutes in PBS, the secondary antibody was applied at 1:500 dilution for 60 minutes at room temperature. Slides are then washed six times for 15 minutes in PBS. 4′,6-diamidino-2-phenylindole (DAPI) (Sigma) staining (nucleus) at 2 µg/ml for 2 minutes was followed by 5 minutes wash in PBS. Slides are mounted with 50% glycerol in PBS with 1,4-diazabicyclo[2.2.2]octane (DABCO) (Sigma) at 100 mg/ml.

Primary antibodies were Laminin (Rabbit IgG-Abcam-ab11575, Cambridge, UK), Cytokeratin-6 (Rabbit IgG-Covance-PRB-169P, Battlecreek, USA), and ß-Catenin (Rabbit polyclonal-Santa Cruz-SC7199, Santa Cruz, USA), Collagen IV (Rabbit IgG-Abcam-ab6586). Secondary antibodies were anti-rabbit-594 (red) Invitrogen-A21207, Carlsbad, California, anti-rabbit-488 (green) Invitrogen-A21206. Slides were examined on Zeiss Axioplan Photomicroscope, Toronto, Canada, equipped with epifluorescent ultraviolet light and corresponding excitation and barrier filters. Pictures were taken on a Nikon Coolpix4500 digital camera, Minato, Japan or Zeiss microscope with camera.

Masson Trichrome Stain

Slides were stained as per standard protocols: Nuclei—black, Muscle, RBC's, Fibrin—red, Collagen—green [27].

Sirius Red Staining

Slides were stained as per standard protocols. Collagen, reticulin, basement membrane—red, Large fibers—yellow or orange Birefringence, Thin fibers—green birefringence, Nuclei—black, Elastin, Muscle, cytoplasm—yellow [28].

Statistical Analysis

Sample size was chosen prior to the start of this study based on preliminary studies to determine adequate numbers required to reach statistical significance. Sample sizes are noted in the "Results" section and figure legends. The data was subjected to a one-way analysis of variance (ANOVA) using the Prism Graph Pad program. This test compares paired groups with multiple members over time, and any mice that were not measured at every time point were excluded from the analysis. A Student *t* test was also used. Total mice included per group per test are indicated in the figure legends.

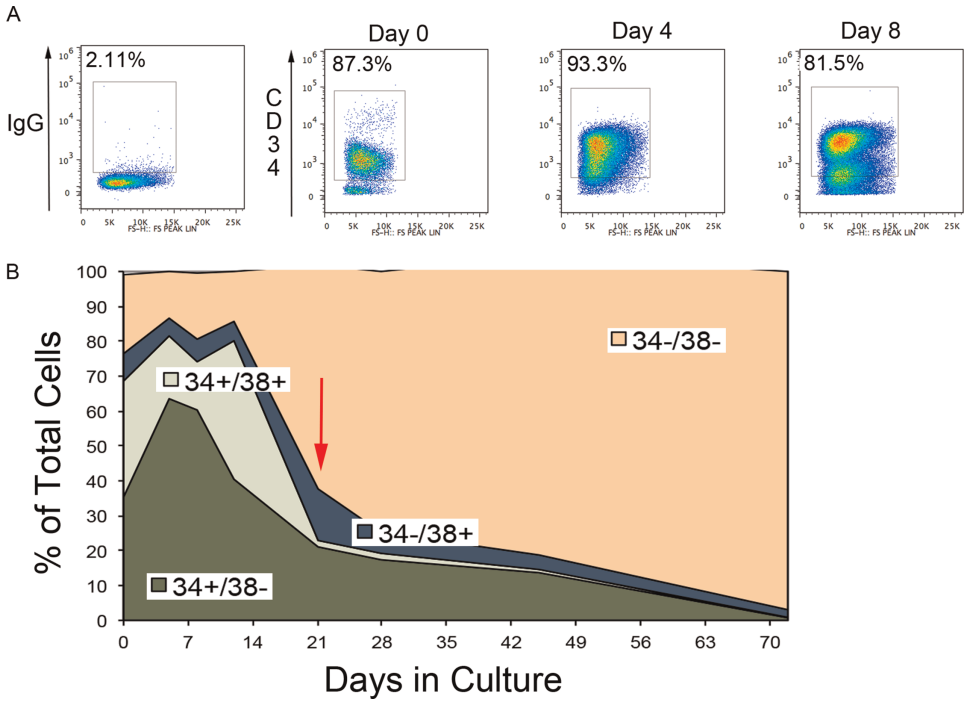

Figure 1. Growth characteristics of CD34+ cells during in vitro culture. CD34+ cells isolated from frozen umbilical cord blood units will proliferate in a defined culture supplemented with FGF4, stem cell factor, and Flt3-ligand. A 100% stacked line graph is used to show the changes in the four populations of cells (CD34+/CD38−, CD34+/CD38+, CD34−/CD38+, CD34−/CD38−). Over time the CD34+ cells are lost during culture. **(A)**: During the first 4–8 days of culture, the enriched population of CD34+ cells was preferentially maintained in culture as observed by an increase in the proportion of CD34+ cells within the population. During this time, the whole population will expand 10-fold. **(B)**: The same trend is shown with a sample group of $n = 10$. The total number of CD34+ cells increases from day 0 to day 7 and were maintained at ∼80% until day 14 and then declined. At day 21 (red arrow), the total CD34+ was ∼40% of the population. By day 70, the proliferation rate has declined and most cells had lost CD34 expression.

A probability (p) value < .05 was considered significant. Test used is indicated in the text.

Results

UCB CD34+ Cell Expansion

The source of UCB units for regenerative medicine will be from the frozen units stored in public and private stem cell banks. This study focused on in vitro cultured CD34+ cells from frozen UCB units. Previously, we have reported on in vitro culture conditions that result in the proliferation of CD34+ cells. Eight days of culture was optimal for maintaining a high frequency of CD34+ cells and an 8- to 10-fold expansion of the total cell population. Data from 10 UCB units showed the column selected CD34+ population had an average frequency of 70% (±20%). This included both CD34+/CD38− and CD34+/CD38+ cells. The double positive cells are considered to be differentiating cells. The CD34+ cells were cultured in an optimized growth media consisting of Stem Span base medium (Stem Cell Technologies), supplemented with FGF4, SCF, and FLT-3L. The growth conditions were developed empirically from a larger set of growth factors. Derivation of the optimized growth conditions have been previously published [12]. The cells in this experiment were grown for a 7–8 day period as this was optimal for the expansion of CD34+ cells. An example of one unit with 87% CD34+ cells maintained high levels of CD34+ cells through to day 8, although by day 8 the frequency of CD34+ cells was declining (Fig. 1A). The growth characteristics of CD34+ cells from 10 UCB units showed that the CD34+ cells peaked at day 7 and were maintained to day 14. The average CD34+ cell content was 70% ± 10% with the CD34+/CD38− cells comprising 55% ± 5% of the total. More mature CD34 cells (CD34+/CD38+) were present at day 14 compared to day 7 indicating that the cells were differentiating in culture. We assumed the CD34+ cells followed the typical reported differentiation pattern so the CD34+/CD38− where the most immature and represented blood progenitor cells, while the CD34+/CD38+ and CD34−/CD38+ were in the lymphoid progenitor group. The double negative cells were maturing lymphoid and myeloid cells. We did not stain for CD33, a marker of myeloid cells here, but we give a more extensive description of the cells in previous reports [12, 13, 21]. The differentiation continued throughout the culture period with a rapid loss of the CD34+ cells as they matured. By day 70, few CD34+ cells were present and the proliferation rate of the whole population also declined (Fig. 1B).

In Vitro Cultured CD34+ Cells Enhance the Rate of Wound Healing

Open skin wounds allow for the application of cells topically and we hypothesized that topical delivery would condition the wound bed and possibly encourage full thickness skin repair. In order to test this hypotheses, a full thickness skin excision wound of 6 mm diameter was made on the back of db/db mice. db/db mice were chosen because they show diabetic

symptoms throughout life such as excessive urination and high blood glucose levels whereas Nonobese Diabetic mice do not develop diabetes until later in life [29]. The excisional wound on the back was prevented from contracting by the addition of a splint. This limited the wound closure to the re-epithelialization of the wound in a manner similar to human wound closure. One million cultured cells were applied to the wound and overlaid with fibrin and tegaderm. The wounds were measured and at the end of the experiment the wound area was excised, fixed and embedded for analysis. A subset of mice was sacrificed at day 3 and day 7 to determine if the cells were still present. Since the db/db mice have a functional immune system and would reject the cells, as expected no cells were present in any of the mice tested at day 7 ($n = 3$).

The topical-applied cells treated group ($n = 25$) showed a faster wound closure compared to the vehicle-control ($n = 23$). Mice terminated at day 7 for histological analysis were excluded from the statistical analysis. The difference in the rate of wound repair for the MPSC group was statistically significant ($p < .05$) for days 3, 7, 10, and 14 post-treatment, confirming that over the 14-day study period the MPSC topical group had faster wound repair compared to the nontreated controls (Fig. 2A).

Our cohort of mice had a range of weights between 34 and 55 g, with the heavier animals in the control group demonstrating slower wound closure compared to the whole group (compare non-cell treated controls in Fig. 2B to Fig. 2A). In order to determine if the MPSC maintained their therapeutic ability for heavier animals with compromised wound regeneration, we analyzed the data from the heavier subgroup (45–50 g) (Fig. 2B). Mice were age matched (12 weeks) and the nontreated control group (45–50 g, $n = 13$) and the MPSC-treated group (45–50 g, $n = 10$) were compared for the rate of wound healing. The MPSC treated group resulted in an accelerated wound closure compared to the nontreated controls. The difference in wound closure rate was significant at day 3, 7, 10, and 14 ($p < .5$).

In a separate study, we compared 1 million BM-mesenchymal stromal cells ($n = 10$) to 1 million MPSC ($n = 15$) and to vehicle controls ($n = 14$). Both the BM-MSC and the MPSC showed statistically significant improvement in the rate of wound healing compared to the controls ($p < .5$). Each cell type enhanced wound closure at a similar rate to each other (Fig. 2C).

Characterization of the Tissue Structure of MPSC Treated Wounds

The rate of wound closure was accelerated in treated animals with 1 million cells and close examination of the wounds indicated that repair-initiated events such as clot formation, neutrophil migration, and keratinocyte migration were similar for both control and UCB treated groups, but the control animals never completed repair of the wounds. Immunohistochemistry of MPSC treated wounds at day 7 reinforced that the wounds were undergoing normal tissue regeneration (Fig. 3). H&E staining and immunofluorescence (IF) labeling of MPSC treated wounds revealed proliferating epidermal cells at the edge of the wounds and migrating across the wound opening. A cross section of the wound stained by H&E (Fig. 3A, 3B) and IF with anti-cytokeratin-6 antibody (Fig. 3C, arrowhead), shows

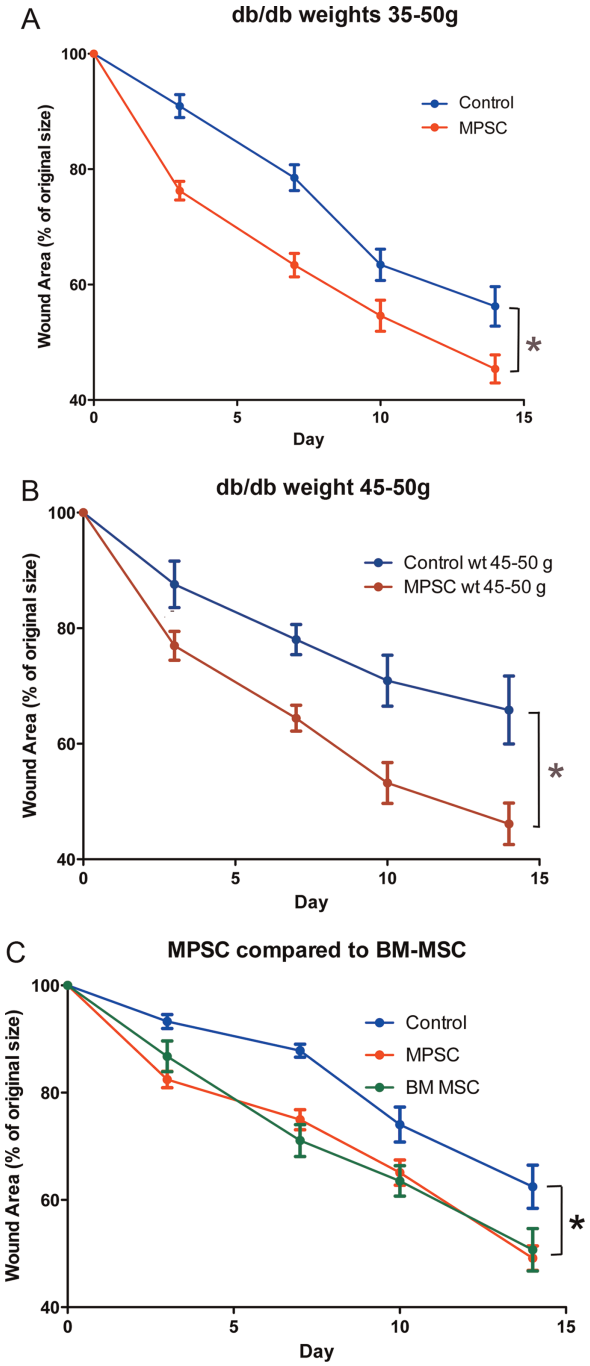

Figure 2. Efficacy of MPSC treatment. Injured mice received MPSCs applied topically to the wound. Control animals were injured but did not receive cells. **(A)**: Topical application of MPSC ($n = 25$) resulted in faster wound closure when compared to controls ($n = 23$) (*, $p < .05$). **(B)**: Analysis of the heavier, diabetic subgroup of db/db mice revealed that the topical applied MPSC ($n = 13$) enhanced wound repair compared to a weight matched control group ($n = 10$), indicating the MPSC work well even within a severe obese environment. **(C)**: Bone marrow MSC ($n = 10$) were compared to MPSC ($n = 15$) and nontreated controls ($n = 14$). The MPSC and BM-MSC showed similar rates of healing and both were significantly different from the controls. Values are expressed as percentage of original wound (100%) ± SEM. *, $p < .05$. p values were determined by two-way ANOVA and Bonferroni post-test. Abbreviations: ANOVA, analysis of variance; BM- MSC, mesenchymal stromal cells from bone marrow; MPSC, multipotential stem cells; MSC, mesenchymal stromal cells.

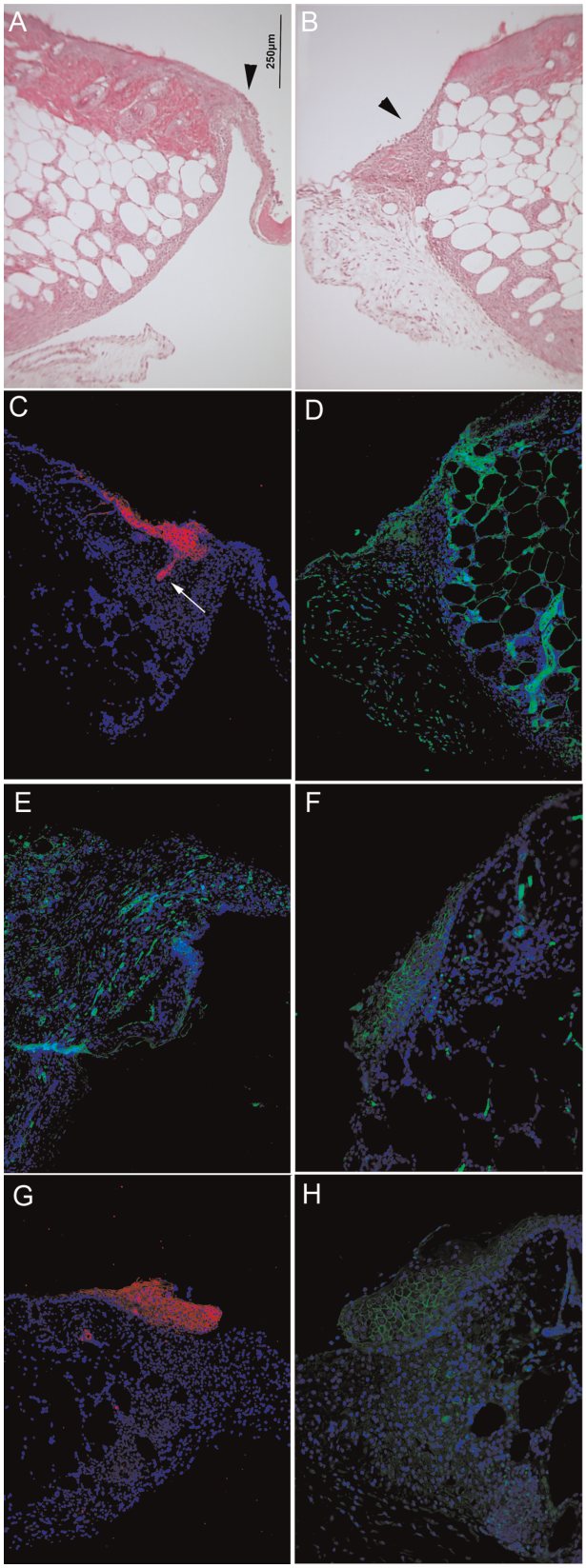

Figure 3.

activated keratinocytes in the hair follicle and accumulating at the wound edge in the proliferation zone.

Within the proliferating zone and the epithelial tongue stretching across the wound, we observed ECM and basement membrane proteins in the UCB treated wounds. Collagen IV, a basement membrane protein, was observed in new tissue being produced at the wound edge and underlying the migrating keratinocytes (Fig. 3D). Lamina, another basement membrane protein that is also found in the ECM during wound repair, can be observed in the epithelial tongue in the migrating keratinocytes as well as in the underlying connective tissue layer (Fig. 3E).

We also observed ß-catenin expression overlapping with the proliferating and migrating epithelial cells. Increased levels of ß-catenin normally are found in the maturing keratinocytes as observed for the MPSC treated wounds (Fig. 3F). Non-treated wounds (control) demonstrated similar IF staining patterns for Cytokeratin-6 and ß-Catenin as the MPSC treated wounds at day 7 (Fig. 3G, 3H).

However, wound repair is not sustained in the nontreated group based on inferior wound repair observed at days 14–23 when compared to that of the UCB-treated group (Fig. 4). At day 7, the control and UCB treated wounds displayed a thickening around the wound edge with the UCB group demonstrated an advancing band of cells (Fig. 4A). At day 23, the wounds were excised and placed onto a black surface and photographed. On day 23, wounds in both groups were fully covered; however, the wound gap in the control was thin and almost transparent whereas the gap in the MPSC treated wound was thick and solid (Fig. 4B).

Histological analysis of representative tissue from controls and topical MPSC on day 23, using H&E, Mason Trichrome and Sirius Red staining, revealed a spectrum of tissue regeneration. We also include mice treated with MPSC but the 1 million cells were injected around the perimeter of the wound in four places (Fig. 5). These mice acted as controls as they received cells that were in close proximity to the wound but the cells were not in contact with the wound bed. The injected-treated

Figure 3. Protein expression indicating the activation of keratinocytes and granulation tissue formation was observed in multipotential stem cells (MPSC) treated wounds. **(A, B)**: Cross section of a topical MPSC treated wound (1 million cells) stained with H&E at day 7 reveals keratinocytes migrating across the wound and underlying extracellular matrix (ECM) formation (arrowhead). **(C)**: A serial section of the same tissue stained with an anti-Cytokeratin-6 antibody with a red fluorescent secondary antibody shows the induction of Cytokeratin-6 (red) expression in activated keratinocytes observed in the hair follicle (arrow) and the proliferating basal layer. **(D)**: Collagen IV (green-fluorescent secondary antibody) is observed in proximity to the fibroblasts in the granulation tissue. **(E)**: Laminin (green-fluorescent secondary antibody), a component of the ECM in healthy skin, is expressed by keratinocytes and fibroblasts during wound healing and can be seen throughout the new tissue being produced. **(F)**: ß-catenin (green-fluorescent secondary antibody) is also expressed by activated keratinocytes and is expressed in a pattern similar to Cytokeratin-6. **(G, H)**: The control mice at day 7 also demonstrated Cytokeratin-6 (red-fluorescent secondary antibody) and ß-Catenin (green-fluorescent secondary antibody) staining. The day 7 control wounds display a similar pattern as topical MPSC treated wounds at day 7. Despite similar initiation of wound repair, the regeneration of the control tissue is not sustained, as tissue samples on day 23 did not show the same rate of wound closure as MPSC-treated wounds. (Refer to Fig. 1). Magnification is the same for all pictures. Bar = 250 μm.

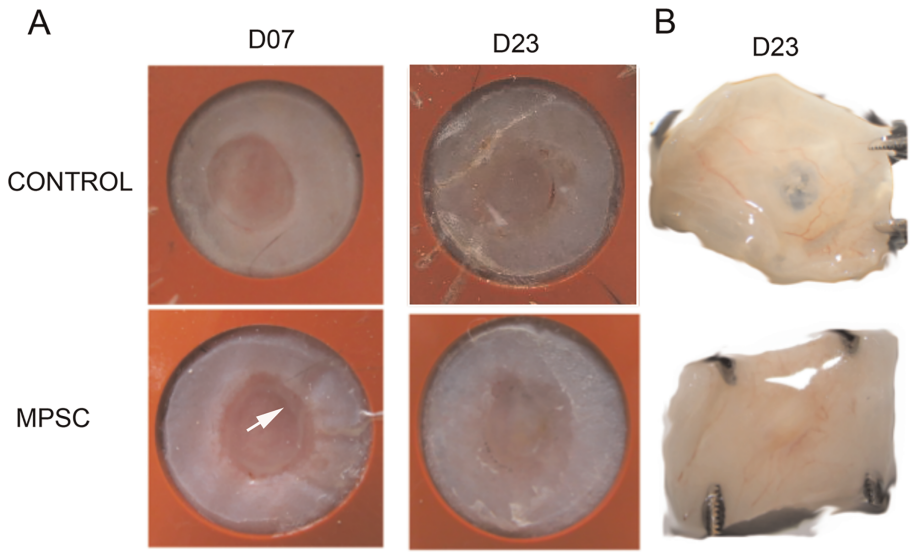

Figure 4. Gross tissue analysis of wounds at day 23 reveals a difference in the quality of the new tissue. Full thickness skin wounds were generated using a 6 mm biopsy punch. The wound was allowed to heal through re-epithelialization by the addition of a splint to prevent the wound edges from migrating together. **(A)**: A white plaque of tissue (considered advancing epithelial tissue) is evident in the wound edge at day 7 for the MPSC treated wound (arrow). At day 23, both control and treated wounds are fully covered. **(B)**: Wounds were excised at day 23 and photographed on a black background. For the control wound, the black background could be observed at the center of the wound indicating a thin covering while for the MPSC treated wound the black background is not observed indicating a thicker layer of tissue. Abbreviation: MPSC, multipotential stem cells.

mice failed to enhance wound closure and were similar to the controls (Supporting Information Fig. S1). The nontreated wound and the MPSC injected wounds looked similar. A keratin layer was observed over a thick epidermis layer. The underlying dermis was thick and exuberant in both groups, consisting of a thick layer fibroplasia characterized by numerous fibroblasts/fibrocytes and collagenous matrix (Fig. 5A, 5B). Neither the nontreated or injected MPSC mice had regenerated hair follicles, sebaceous glands, or panniculus carnosus. In contrast, the MPSC topical treated wounds display a well-organized epidermis and dermis with clusters of epithelial cells that occasionally contain melanin-like pigment, hence were interpreted as regenerating adnexal structures (Fig. 5B-Topical-H&E-arrows). Similar to the uninjured skin, the MPSC topical treated wounds also have reformed the panniculus carnosus and underlying adipose (compare wounds to uninjured skin Fig. 5B).

Discussion

It has been hypothesized that the initiation of epithelial wound repair is due to the activity of endogenous EPC, CAC, and MSC, but these cells from patients with tissue ischemia have a reduced capacity to initiate tissue repair and this incapacitation is further aggravated in elderly patients and patients with diabetes. Nonhealing skin wounds experienced by type 2 diabetic patients can progress to amputation or death if not treated properly. The proper management of T2DM will slow down the progression of skin ulcers and tissue ischemia but for advanced disease there are limited options. Current treatment procedures for chronic wounds include debridement, reduce pressure on weight bearing wounds, the use of dressing, including ones that contain ECM proteins and in severe cases, skin grafting or tissue flaps are used [30, 31].

In this report, we tested the regeneration capacity of MPSC from UCB in a mouse model where the cells are present for a limited time. db/db mice provided us with a diabetic environment in a fully functional immune system thus making the diabetic wound model similar to an unmatched allogeneic setting for human patients. This model allows for the determination of the tissue regeneration properties of MPSC by the paracrine signaling mechanism only as unmatched cells are eventually eliminated by the mouse immune system.

MPSC Demonstrate Therapeutic Properties in an Unmatched Model of Diabetic Wound Healing

Studies have indicated that using healthy, young donor cells would result in better tissue repair than using autologous cells from the patient. Thus, determining the validity of using allogeneic cell-based therapies for the treatment of nonhealing wounds is required. Animal models of limb or cardiac ischemia and human clinical trials have determined that disease and age can adversely affect the efficacy of autologous cells used for treatment. Using a hind limb femoral artery ligation model, Zhou et al. [24] demonstrated that cells from aged rats had a 50% reduction in EPC and a comparable reduction in levels of vascular endothelial growth factor (VEGF) and bFGF. Sugihara et al. [32] demonstrated that aged mice developed a decreased neovascularization response to ischemia compared to young mice due to a decrease in the migratory capacity of their monocytes. The transplantation of young BM cells into old mice with hind limb ischemia improved both neovascularization and increased VEGF levels resulting in improved blood flow [33, 34]. Another study found that patients with critical limb ischemia had reduced EPC in their peripheral blood compared with healthy individuals [35]. Similar findings have been reported from patients with diabetes [22, 36].

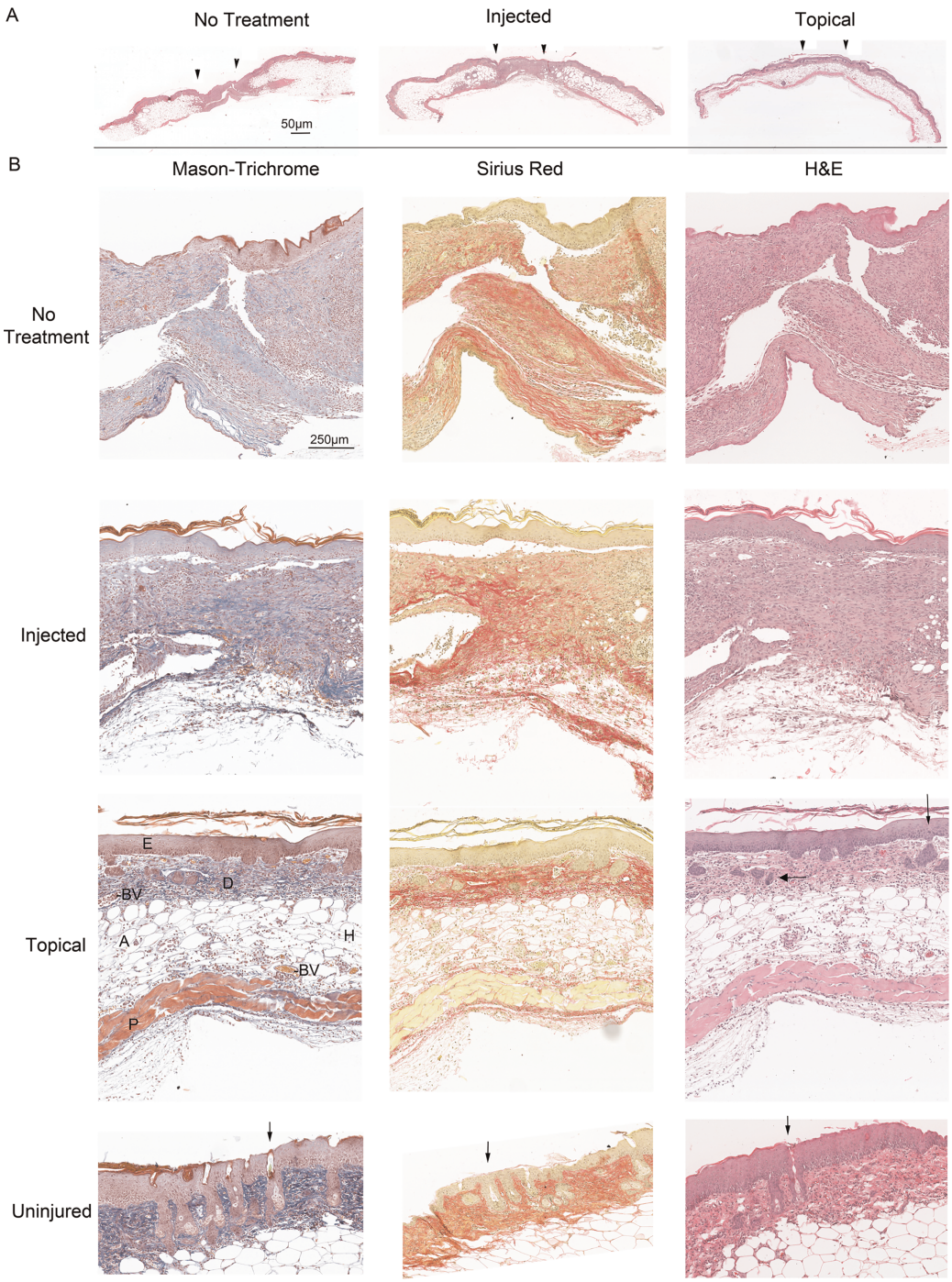

Figure 5. Topical application of multipotential stem cells (MPSC) results in a better quality regeneration of the skin. Histological analysis of the wounds demonstrated that topical MPSC treated wounds result in superior healing compared to injected MPSC and controls. **(A)**: Comparison of wounds harvested at day 23 from no treatment (control), injected MPSC and topical applied MPSC, demonstrate better skin architecture for the topical treated wounds. Arrows depict wound edges. Both no-treatment and injected have a thick epidermis and fibroplasia in the dermis (compare to the Topical treated skin-H&E stain) Bar = 50 μm. **(B)**: Mason-Trichrome stain displays Keratin (red), Collagen (blue), Erythrocytes (orange), and Muscle (red). Sirius Red staining displays Keratin (yellow), Collagen (red), Erythrocytes (yellow), and Muscle (yellow). At day 23 postinjury the amount of cytokeratin, by visual observation, is similar between all three treatment groups, but the remodeling of the wound is more advanced in the topical treated wound with the appearance of organized layers of epidermis (E), dermis (D), hypodermis (H) including adipose (A), panniculus carnosus (P) blood vessels (BV), and regenerating hair follicles (arrows-H&E). The control and injected group also lack the panniculus carnosus layer, blood vessels and have no regenerating hair follicles. Comparing the topical treated skin to uninjured skin reveals that nascent hair follicles (arrows-H&E) are forming in the topical treated wounds indicating that by day 23 tissue remodeling is not complete. Bar = 250 μm.

Although many studies have determined that specific cells within our bodies have the ability to induce tissue regeneration, we can only use this ability to a limited extent. When tissue specific stem or progenitor cells that are responsible for normal tissue homeostasis are transplanted into damaged or ischemic tissue, they initiate regeneration. This suggests that the properties of the niche remain intact and can sustain tissue repair and that in disease states such as diabetes, the rate-limiting step maybe the intrinsic properties of the resident tissue stem or progenitor cells [4, 23, 37–39]. This is supported by our previous study where we used MPSC to treat PVD in Non obese diabetic/severe combined imunnodeficient (NOD/SCID) mice. In that study, the mice did not reject the human MPSCs so both paracrine signaling and engraftment and differentiation of the MPSC occurred. We observed increased blood flow and vascularization in the treated animals with some of the new tissue composed of human cells. Taken together, both direct engraftment and paracrine signaling from the MPSC contributed to tissue regeneration [21].

Although UCB is a potential source of therapeutic CAC, MSC, and EPC [16, 40, 41] that contribute to tissue regeneration through paracrine signaling and engraftment, our model of diabetic wound healing using unmatched donor cells allows only the paracrine signaling to be effective. MPSC secrete a wide range of chemokines and cytokines. Our previous studies demonstrated that the most abundantly secreted factors are ones that reduce inflammation, increase vascularization, and are anti-apoptotic [21].

Quality of Wound Healing

In order to properly assess the therapeutic effect of MPSC, we considered the strain of the mouse used and the disease being treated. db/db mice on a C57Bl/6 background is a standard model for investigating the ability of donor cells to enhance diabetic wound healing [42]. Using human cells and db/db mice that have a fully functioning immune system was analogous to an unmatched human diabetic model. Analyzing with an antibody to human mitochondria to detect human cells, we demonstrated that although the MPSC were rejected within ~7 days as expected (data not shown), the cells still had a significant positive effect on wound healing similar to our previous observation using MPSC to treat spinal cord injury, PVD, and bone regeneration [21, 25, 26].

Microscopic assessment of tissue sections from day 7, 14, and 23 control and MPSC treated mice revealed key protein expression and distribution patterns that indicate the addition of MPSC improves the rate and quality of the new tissue. The MPSC treated tissue was organized into multiple layers indicative of normal skin architecture. In contrast, nontreated wounds were covered by a thin layer of epidermis (day 7) and a thick layer of dermis consistent with fibroplasia (fibroblasts and Collagen) without organization (day 23).

IF analysis of the wounds revealed that the MPSC supported the normal mechanism of wound repair as demonstrated by the presence of ß-catenin, Laminin, Cytokeratin-6, and Collagen IV. During wound repair, intracellular calcium levels regulate the activation of immature keratinocytes in the hair follicle by activating the wnt/ß-catenin signaling path, which induced the keratinocytes to migrate from the hair follicle to the edge of the wound [43]. Analysis of the wounds by IF revealed that ß-catenin is expressed in the proliferating zone-epidermal cells at the wound edge and in the epithelial tongue. The activated keratinocytes also express Cytokeratin-6. Cytokeratin-6 is not expressed in healthy skin but during wound healing the normally nonproliferating epidermal cells in the spinous and granulous layers will express cytokeratin-6. The activated keratinocytes appear to originate from the hair follicle [44, 45] as observed in our study and migrate to the wound edge to form a thick epidermal layer over the newly formed granulated tissue.

Below the keratinocyte layer were proliferating fibroblasts that produce basement membrane and ECM proteins that form the bases of new granulation tissue. The basement membrane is a layer of specialized ECM that separates the epidermis from the dermis and normally expresses a unique set of proteins. Laminin is only found in the basement membrane in healthy skin but during wound healing both keratinocytes and fibroblasts produce Laminin which is deposited in the basement membrane and the ECM as observed in the MPSC treated wounds at day 7. Over time the ECM is remodeled and Laminin is then found restricted to the basement membrane. Laminin has important roles in wound healing that include providing structure for the new skin, anti-microbial activity and Laminin acts as a chemoattractant for monocytes and promotes keratinocyte migration during the early stages of wound regeneration [46]. The fibroblasts also produce Collagens that are a main source of ECM proteins of granulation tissue. Similar to Laminin, the ECM and basement membrane have distinct Collagen compositions. Collagen I is a component of the ECM while Collagen IV is found in the basement membrane and has a role in keratinocyte growth and differentiation. Studies have demonstrated that Collagen IV has a role in promoting normal skin organization [47, 48]. Studies that plated human keratinocytes on polycarbonate coated with Collagen IV, demonstrated that polarized epithelial tissue was formed including a spinous layer, a thin layer of stratum granulosum and stratum corneum. When Collagen I, which is not a component of the BM was used as a coating, the formed tissue was less organized and did not develop fully. This emphasizes the importance of Collagen IV in the development of organized tissue during wound regeneration [49], as we have observed in MPSC treated wounds at day 7. All of the controls consisted of media (no cells) overlaid with Fibrin that could possibly act as a scaffold for endogenous migrating neutrophils and keratinocytes, but surprisingly, on its own, did not provide the same therapeutic benefit as when MPSCs were present.

Conclusion

We have demonstrated that placing MPSC directly on the wound, compared to nontreated controls, resulted in superior tissue regeneration. Furthermore, use of an unmatched model demonstrated that MPSC could initiate tissue regeneration that is maintained after the cells are eliminated; hence underlying the importance of paracrine signaling. Although both direct engraftment and paracrine signaling mechanisms contribute to tissue regeneration, paracrine signaling from MPSC can lead to improved healing even when it is the only mechanism available. Furthermore, expansion of cells during the production of MPSC could result in a sufficient number of cells for multiple treatments from a single UCB unit. Since we are able

to achieve a 10-fold expansion of cells during an 8-day culture, an average cord blood collection would generate over 10^9 MPSC, which would be adequate for the treatment of up to three hundred 1-cm^2 wounds [7, 11, 25, 50].

Acknowledgments

Umbilical cord blood and tissue collections: Research Centre for Women's and Infants' Health, Lunenfeld-Tanenbaum Research Institute, Mount Sinai Hospital, Toronto, Canada, http://biobank.lunenfeld.ca. The authors acknowledge the histology assistance from the Lunenfeld-Tanenbaum Research Institute's CMHD Pathology Core (www.cmhd.ca). Graphical Abstract drawn by Kayla Hoffman-Rogers (khoffmanrogers@gmail.com). This study was funded by CIHR-PPP110824, Center for the Commercialization of Regenerative Medicine-001, Insception-LifeBank-003, and Stem Cell Network-13/5226 (CT74). H.A. is currently affiliated with the Molecular Pathology Unit, Laboratory of Cancer Biology and Genetics, Center for Cancer Research, National Cancer Institute, Bethesda, MD.

Author Contributions

J.W. and T.C. conception and design, and/or assembly of data, data analysis and interpretation, manuscript writing. H.A. data analysis and manuscript writing. A.K. data analysis and manuscript writing. I.M.R. conception and design, and/or assembly of data, data analysis and interpretation, manuscript writing, final approval of manuscript.

Disclosure of Potential Conflicts of Interest

I.M.R. is a scientific advisor and has received research funding from Insception Lifebank. The other authors indicated no potential conflicts of interest.

References

1 Singer AJ, Clark RA. Cutaneous wound healing. N Engl J Med 1999;341:738–746.

2 Koh TJ, DiPietro LA. Inflammation and wound healing: The role of the macrophage. Expert Rev Mol Med 2011;13:e23.

3 Baltzis D, Eleftheriadou I, Veves A. Pathogenesis and treatment of impaired wound healing in diabetes mellitus: New insights. Adv Ther 2014;31:817–836.

4 Schatteman GC, Hanlon HD, Jiao C et al. Blood-derived angioblasts accelerate blood-flow restoration in diabetic mice. J Clin Invest 2000;106:571–578.

5 Sivan-Loukianova E, Awad OA, Stepanovic V et al. CD34+ blood cells accelerate vascularization and healing of diabetic mouse skin wounds. J Vasc Res 2003;40:368–377.

6 Mason RM, Wahab NA. Extracellular matrix metabolism in diabetic nephropathy. J Am Soc Nephrol 2003;14:1358–1373.

7 Wu Y, Chen L, Scott PG et al. Mesenchymal stem cells enhance wound healing through differentiation and angiogenesis. Stem Cells 2007;25:2648–2659.

8 O'Loughlin A, Kulkarni M, Vaughan EE et al. Autologous circulating angiogenic cells treated with osteopontin and delivered via a collagen scaffold enhance wound healing in the alloxan-induced diabetic rabbit ear ulcer model. Stem Cell Res Ther 2013;4:158.

9 Elsharawy MA, Naim M, Greish S. Human CD34+ stem cells promote healing of diabetic foot ulcers in rats. Interact Cardiovasc Thorac Surg 2012;14:288–293.

10 van der Strate BW, Popa ER, Schipper M et al. Circulating human CD34+ progenitor cells modulate neovascularization and inflammation in a nude mouse model. J Mol Cell Cardiol 2007;42:1086–1097.

11 Rogers I, Sutherland DR, Holt D et al. Human UC-blood banking: Impact of blood volume, cell separation and cryopreservation on leukocyte and CD34(+) cell recovery. Cytotherapy 2001;3:269–276.

12 Rogers I, Yamanaka N, Bielecki R et al. Identification and analysis of in vitro cultured CD45-positive cells capable of multilineage differentiation. Exp Cell Res 2007;313:1839–1852.

13 Rogers IM, Yamanaka N, Casper RF. A simplified procedure for hematopoietic stem cell amplification using a serum-free, feeder cell-free culture system. Biol Blood Marrow Transplant 2008;14:927–937.

14 Falanga V, Iwamoto S, Chartier M et al. Autologous bone marrow-derived cultured mesenchymal stem cells delivered in a fibrin spray accelerate healing in murine and human cutaneous wounds. Tissue Eng 2007;13:1299–1312.

15 Mareschi K, Biasin E, Piacibello W et al. Isolation of human mesenchymal stem cells: Bone marrow versus umbilical cord blood. Haematologica 2001;86:1099–1100.

16 Erices A, Conget P, Minguell JJ. Mesenchymal progenitor cells in human umbilical cord blood. Br J Haematol 2000;109:235–242.

17 Kern S, Eichler H, Stoeve J et al. Comparative analysis of mesenchymal stem cells from bone marrow, umbilical cord blood or adipose tissue. Stem Cells 2006;24:1294–1301.

18 Bieback K, Kern S, Kluter H et al. Critical parameters for the isolation of mesenchymal stem cells from umbilical cord blood. Stem Cells 2004;22:625–634.

19 Barclay GR, Tura O, Samuel K et al. Systematic assessment in an animal model of the angiogenic potential of different human cell sources for therapeutic revascularization. Stem Cell Res Ther 2012;3:23.

20 Vanneaux V, El-Ayoubi F, Delmau C et al. In vitro and in vivo analysis of endothelial progenitor cells from cryopreserved umbilical cord blood: Are we ready for clinical application? Cell Transplant 2010;19:1143–1155.

21 Whiteley J, Bielecki R, Li M et al. An expanded population of CD34+ cells from frozen banked umbilical cord blood demonstrate tissue repair mechanisms of mesenchymal stromal cells and circulating angiogenic cells in an ischemic hind limb model. Stem Cell Rev 2014;10:338–350.

22 Fadini GP, Miorin M, Facco M et al. Circulating endothelial progenitor cells are reduced in peripheral vascular complications of type 2 diabetes mellitus. J Am Coll Cardiol 2005;45:1449–1457.

23 Fadini GP, Sartore S, Albiero M et al. Number and function of endothelial progenitor cells as a marker of severity for diabetic vasculopathy. Arterioscler Thromb Vasc Biol 2006;26:2140–2146.

24 Zhuo Y, Li SH, Chen MS et al. Aging impairs the angiogenic response to ischemic injury and the activity of implanted cells: Combined consequences for cell therapy in older recipients. J Thorac Cardiovasc Surg 2010;139:1286–1294.

25 Chua SJ, Bielecki R, Yamanaka N et al. The effect of umbilical cord blood cells on outcomes after experimental traumatic spinal cord injury. Spine 2010;35:1520–1526.

26 Tam V, Rogers I, Chan D et al. A comparison of intravenous and intradiscal delivery of multipotential stem cells on the healing of injured intervertebral disk. J Orthop Res 2014;32:819–825.

27 Bancroft J. Theory and Practice of Histological Techniques. Elsevier Health Sciences, Amsterdam, Netherlands, 2008:1008.

28 Toki D, Zhang W, Hor KL et al. The role of macrophages in the development of human renal allograft fibrosis in the first year after transplantation. Am J Transplant 2014;14:2126–2136.

29 Labs J. Available at https://www.jax.org/strain/000697. Accessed April 17, 2018.

30 Snyder RJ, Shimozaki K, Tallis A et al. A prospective, randomized, multicenter, controlled evaluation of the use of dehydrated amniotic membrane allograft compared to standard of care for the closure of chronic diabetic foot ulcer. Wounds 2016;28:70–77.

31 Kallio M, Vikatmaa P, Kantonen I et al. Strategies for free flap transfer and revascularisation with long-term outcome in

the treatment of large diabetic foot lesions. Eur J Vasc Endovasc Surg 2015;50:223–230.

32 Sugihara S, Yamamoto Y, Matsuura T et al. Age-related BM-MNC dysfunction hampers neovascularization. Mech Ageing Dev 2007;128:511–516.

33 Peng C, Chen B, Kao HK et al. Lack of FGF-7 further delays cutaneous wound healing in diabetic mice. Plast Reconstr Surg 2011;128:673e–684e.

34 Guo R, Chai L, Chen L et al. Stromal cell-derived factor 1 (SDF-1) accelerated skin wound healing by promoting the migration and proliferation of epidermal stem cells. In Vitro Cell Dev Biol Anim 2015;51:578–585.

35 Smadja DM, Duong-van-Huyen JP, Dal Cortivo L et al. Early endothelial progenitor cells in bone marrow are a biomarker of cell therapy success in patients with critical limb ischemia. Cytotherapy 2012;14:232–239.

36 Caballero S, Sengupta N, Afzal A et al. Ischemic vascular damage can be repaired by healthy, but not diabetic, endothelial progenitor cells. Diabetes 2007;56:960–967.

37 Klibansky DA, Chin A, Duignan IJ et al. Synergistic targeting with bone marrow-derived cells and PDGF improves diabetic vascular function. Am J Physiol Heart Circ Physiol 2006;290:H1387–H1392.

38 Tan Q, Qiu L, Li G et al. Transplantation of healthy but not diabetic outgrowth endothelial cells could rescue ischemic myocardium in diabetic rabbits. Scand J Clin Lab Invest 2010;70:313–321.

39 Schmieder RE. Endothelial dysfunction: How can one intervene at the beginning of the cardiovascular continuum? J Hypertens Suppl 2006;24:S31–S35.

40 Finney MR, Greco NJ, Haynesworth SE et al. Direct comparison of umbilical cord blood versus bone marrow-derived endothelial precursor cells in mediating neovascularization in response to vascular ischemia. Biol Blood Marrow Transplant 2006;12:585–593.

41 Baker CD, Balasubramaniam V, Mourani PM et al. Cord blood angiogenic progenitor cells are decreased in bronchopulmonary dysplasia. Eur Respir J 2012;40:1516–1522.

42 Michaels J, Churgin SS, Blechman KM et al. db/db mice exhibit severe wound-healing impairments compared with other murine diabetic strains in a silicone-splinted excisional wound model. Wound Repair Regen 2007;15:665–670.

43 Cheon SS, Wei Q, Gurung A et al. Beta-catenin regulates wound size and mediates the effect of TGF-beta in cutaneous healing. FASEB J 2006;20:692–701.

44 Laplante AF, Moulin V, Auger FA et al. Expression of heat shock proteins in mouse skin during wound healing. J Histochem Cytochem 1998;46:1291–1301.

45 Wojcik SM, Bundman DS, Roop DR. Delayed wound healing in keratin 6a knockout mice. Mol Cell Biol 2000;20:5248–5255.

46 Senyurek I, Kempf WE, Klein G et al. Processing of laminin alpha chains generates peptides involved in wound healing and host defense. J Innate Immun 2014;6:467–484.

47 Abreu-Velez AM, Howard MS. Collagen IV in normal skin and in pathological processes. N Am J Med Sci 2012;4:1–8.

48 Yang SW, Geng ZJ, Ma K et al. Comparison of the histological morphology between normal skin and scar tissue. J Huazhong Univ Sci Technol Med Sci 2016;36:265–269.

49 Segal N, Andriani F, Pfeiffer L et al. The basement membrane microenvironment directs the normalization and survival of bioengineered human skin equivalents. Matrix Biol 2008;27:163–170.

50 Javazon EH, Keswani SG, Badillo AT et al. Enhanced epithelial gap closure and increased angiogenesis in wounds of diabetic mice treated with adult murine bone marrow stromal progenitor cells. Wound Repair Regen 2007;15:350–359.

See www.StemCellsTM.com for supporting information available online.